Bidirectionality From Cargo Thermal Fluctuations in Motor-Mediated Transport

Christopher E. Miles, James P. Keener
Department of Mathematics, University of Utah

miles@math.utah.edu

May 16, 2022

Abstract

Molecular motor proteins serve as an essential component of intracellular transport by generating forces to haul cargoes along cytoskeletal filaments. Two species of motors that are directed oppositely (e.g. kinesin, dynein) can be attached to the same cargo, which is known to produce bidirectional net motion. However, the mechanism of switching remains subtle. Although previous work focuses on the motor number as the driving noise source for switching, this work proposes an alternative possibility: cargo diffusion. A mean-field mathematical model of mechanical interactions of two populations of molecular motors with cargo thermal fluctuations (diffusion) is presented to study this phenomenon. The delayed response of a motor to fluctuations in the cargo velocity is quantified, allowing for the reduction of the full model a single "characteristic position", a proxy for the net force on the cargo. The system is then found to be metastable, with switching exclusively due to cargo diffusion between two distinct directional transport states. The time to switch between these states is then investigated using a mean first passage time analysis. The switching time is found to be non-monotonic in the drag of the cargo, providing an experimental prediction for verification.

1. INTRODUCTION

Active transport is a key component of cellular function due to the compartmental nature of cellular machinery. This transport is achieved through the use of molecular motor proteins, which undergo a series of conformational changes to walk along cytoskeletal filaments and generate forces to haul cargoes [10]. The transport of a single cargo can often involve two families of motors that are directed oppositely, denoted *bidirectional transport* [8]. For instance, kinesin, which walks in the positive direction of a microtubule, and dynein, which walks in the negative direction, can be attached to the same cargo. Another possibility is that two populations of the same family of kinesin motor can be attached to a cargo but walk along oppositely oriented microtubule tracks [26]. This phenomenon is observed for a variety of cargoes: mRNA particles, virus particles, endosomes, and lipid droplets [9, 16]. Although both families of motors are exerting forces on the cargo in opposite directions, the direction of cargo transport is able to switch directions [1]. That is, the cargo spends periods of time with a net positive, negative, and zero velocity (denoted a pause state). This distinct switching suggests a mechanism of *cooperation* between the motor families that has been explored from both experimental and theoretical perspectives.

The role of external influences in the cooperation mechanism remains unclear. A number of studies have identified regulators of kinesin and dynein [4]. For instance, LIS1 and NudE have

been found to modulate dynein's force production capabilities [22]. In [28], the authors found that the microtubule itself can regulate kinesin force production. However, the necessity of these external regulators for motor coordination in bidirectional transport remains unestablished. The alternative hypothesis relies on the notion that the coordination is a product of the mechanical interactions of the motors with the cargo, denoted a *tug-of-war* scenario.

The tug-of-war hypothesis has also been investigated from a theoretical and experimental perspective. The authors in [24] formulate the most notable mathematical model capable of producing bidirectionality. In the model, the motors share the load equally. This assumption is not always invoked in later mathematical models. For instance, [17] performs stochastic simulations of unequally distributed motors. However, these authors compare the results of the stochastic simulation with experiments and conclude that switching statistics do not match as the number of motors varies. In [29], another mathematical model is proposed where the two motor populations are required to be asymmetric. That is, the two opposing motor populations must have different force generating properties to break symmetry. [19, 20] also provide noteworthy mathematical models, thinking of motor transport as a "rubber-band"-like process. In [2], the authors reexamine the mathematical model of [17] and stress the importance of cargo diffusion for the model to produce the right behavior.

In this work, we present a new tug-of-war model of bidirectional motor-mediated transport. Our proposed model contains fundamentally different essential components than previous work. Broadly, the proposed model is a mean-field model with unequally distributed load. This differs from previous discrete motor, unequal load descriptions and therefore requires a different source of noise to induce switching. By examining the dynamics of a single motor, we quantify the delayed response to instantaneous changes in the cargo velocity. An approximation is then made about how this behavior expands to an ensemble of motors, allow for the reduction of the system to two "characteristic positions", one for each motor population. We verify this approximation is valid with numerical simulations of a single population. In the two-variable system, we find metastability with two states corresponding to positive and negative net velocities, or bidirectional motion. The noise that drives switching between these two states is due to cargo diffusion (thermal fluctuations), an aspect of this process previously noticed but under-emphasized until recent works [2].

Previous work has indeed illustrated the significance of motor number fluctuations [25]. However, in this work, we choose to use a mean-field model to emphasize the lack of necessity of discrete motor number for bidirectionality. The proposed model still incorporates binding and unbinding dynamics and therefore has the same *mean* behavior as a discrete motor model, but lacks the noise associated with discrete events. The only remaining noise source is then cargo diffusion, which we show to be sufficient for bidirectionality. The difference in magnitudes between the fluctuations due to motor number and cargo diffusion is difficult to quantify due to the fundamental difference in structure. In [7], the authors find that motor number fluctuations can result in an effective diffusion when the number of motors involved in transport is large.

A characteristic quantity in validating bidirectional transport models is the reversal or switching time of the system: the time between runs of each direction. In our model, the correlation structure of the effect of noise on each population allows for the reduction to a 1 dimensional mean first passage time problem in a double-well potential. Classical tools can then be used to solve and approximate the corresponding boundary value problem. The switching time is

considered as a function of the cargo drag, which has complex behavior due to the steepening of the wells and strengthening of the diffusion as the drag decreases. Ultimately, the mean switching time is found to be non-monotonic as a function of the cargo drag coefficient, which provides an experimental prediction to validate our diffusion-driven switching hypothesis.
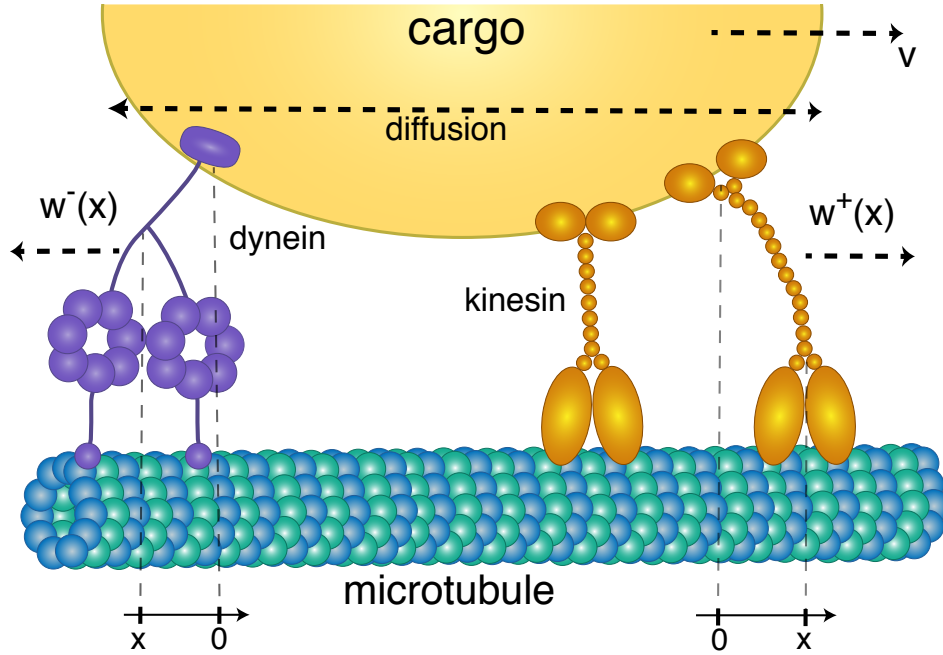
1.1. Model Formulation

Figure 1: A diagram of the mean-field model setup. The quantity, x, denoting the distance a motor is stretched is always measured with respect to the orientation of the microtubule.

Consider a cargo being pulled by two different populations of motors, denoted $+$ and $-$. Let $m^\pm(x, t)$ be the density of type $+$ or $-$ motors at time t and stretched from their unstretched position x units. The $+$ or $-$ labeling of the motor families denotes their preferred directionality. That is, m^+ corresponds to the density of motors preferring to walk in the positive direction (e.g. kinesin) and m^- the density of motors preferring to walk in the negative direction (e.g. dynein). The evolution of each motor population is then described by

$$\frac{\partial m^\pm}{\partial t} + \underbrace{\frac{\partial}{\partial x}\left\{\left[w^\pm(x) - v(t)\right]m^\pm\right\}}_{\text{stepping}} = \underbrace{\left(M^\pm - \int_{-\infty}^{\infty} m^\pm(x, t)\,\mathrm{d}x\right)\Omega_{\text{on}}^\pm(x)}_{\text{binding}} - \underbrace{\Omega_{\text{off}}^\pm(x)m^\pm(x, t)}_{\text{unbinding}}. \qquad (1)$$

Although (1.1) appears as only one equation, m^+ and m^- each have their own equation that are structurally identical but may contain different parameters or functional forms. The quantity x, describing the distance the motor is stretched from its unstretched position is always measured with respect to the microtubule, even though each motor type walks in a different direction,

see **Figure 1**. This choice of frame of reference is convenient, as it causes the two equations to be structurally identical (as opposed to having to reverse the sign of v).

It is worth noting that this PDE has been studied in other contexts, referred to as the Lacker-Peskin PDE [30], which is an extension of the Huxley crossbridge model [11, 13]. In that literature, the particular form of the PDE is derived from the limit of a large number of discrete binding sites. If we consider the case where $M = 1$, the mean field model (1.1) would describe probability density description of a single motor. However, due to the linearity of the equation in M, the description of a population of motors is structurally the same but with $M > 1$.

Before describing, in detail, each term in (1.1), we state a driving assumption for several of the functional forms appearing in the equation. The force generated due to the linker stretching is assumed to be Hookean, that is force $\sim kx$, where k is the spring constant or stiffness of the motor linker attachment to the cargo. The force-displacement curve of molecular motors has been studied experimentally [12, 18] and, although not perfectly linear, seems to be well-approximated by this assumption.

We now discuss each term of the equation in more detail. Broadly, the motor population can change three ways: motors stepping (walking), binding or unbinding.

1. **stepping**: We assume that the rate of stepping of the motor is dependent on the force exerted on the motor, which is some function of the distance between the motor and the cargo based on the Hookean force assumption previously mentioned. The walking rate $w(x)$ is therefore position dependent. We take the particular functional form

$$w(x) := -ax + b,$$

   where $a > 0$. At $x = 0$, which corresponds to the motor being unstretched, the motor walks with some velocity b. For the $+$ directed motor, for instance, $b > 0$. As the motor walks farther from its unstretched position ($x > 0$), the force exerted on it causes the velocity to decrease until it eventually stalls at $x_{\text{stall}} := b/a$. If $x < 0$, that is, the cargo is ahead in the direction the motor seeks to walk, the velocity is assumed to be greater as the linker exerts a force in the direction of motion of the motor. If $x > x_{\text{stall}}$, then the force exerted by the linker is greater than the stall force, meaning the motor moves opposite its preferred direction.

   This force-velocity curve has been qualitatively observed experimentally [6, 16] in several types of motors, and a (non-linear) version of this functional form has been used in a number of modeling papers [2, 17, 24]. The assumed linearized version allows us to perform analysis on the model.

2. **binding**: The functional form of the binding term is set to be

$$\Omega_{\text{on}}(x) := k_{\text{on}} \, \delta(x),$$

   where k_{on} is the constant describing the rate of binding of a molecular motor to the cargo. The $\delta(x)$ functional form corresponds to the assumption that motors are initially unstretched ($x = 0$) when they bind, thus only binding at $x = 0$. That is, the motors only bind in a non-force-producing state. This assumption can be relaxed (and is for later numerical simulations) to a Gaussian approximation of the delta function.

3. **unbinding**: The unbinding rate of molecular motors has experimentally been found to be related to the force exerted on them [12, 17], however the nature of this dependency is complex and varies from motor to motor. For this reason, we again take the simplest form that still behaves in a way that qualitatively matches experimental results, which is

$$\Omega_{\text{off}}(x) = k_{\text{off}} \ \exp\left\{\frac{k|x|}{F_D}\right\}, \tag{2}$$

where again, the force exerted is assumed to be Hookean ($\sim kx$) and can be exerted in either direction (hence the absolute value). F_D is a characteristic force fit to experimental observations, and k_{off} is the unstretched detachment rate. This can be viewed as a version of Bell's Law, where Bell's Law is related to F_D. The overall behavior of this function establishes that motors detach at a faster rate the farther they are stretched due to the force exerted on their microtubule binding sites.

In [17], the authors account for the stalling of motors and the catch-bond behavior of dynein by taking a non-monotonic dependence on the force, but this piecewise description is not taken here.

We then can define the average force exerted by each motor population, recalling the assumption of a Hookean force,

$$F^{\pm}(t) := \int_{-\infty}^{\infty} k^{\pm} x m^{\pm}(x, t)\, dx. \tag{3}$$

2. MATERIALS AND METHODS

In this section, we discuss the analysis performed on the aforementioned model.

2.1. Steady-State Analysis

This time-dependent force, described by (3) is difficult to compute in practice, so we turn our attention to the steady-state force. We consider the steady state ($dm^{\pm}/dt = 0$ and) behavior of (1.1) with some steady-state velocity $\tilde{v}$, which leads to the pair of equations for the steady state densities $\tilde{m}^{\pm}$

$$\frac{\partial}{\partial x}\left\{\left[w^{\pm}(x) - \tilde{v}\right]\tilde{m}^{\pm}\right\} = \left(M^{\pm} - \int_{-\infty}^{\infty} \tilde{m}^{\pm}(x)\, dx\right)\Omega_{\text{on}}^{\pm}(x) - \Omega_{\text{off}}^{\pm}(x)\tilde{m}^{\pm}(x). \tag{4}$$

Exploiting the linearity of (2.1), along with the partitioning nature of the delta function, (2.1) can be solved analytically, resulting in a solution with an integrable singularity at the stall position dependent on the velocity

$$x_{\text{stall}} := \frac{b - \tilde{v}}{a}.$$

For details of this calculation, see **Supplementary Section S1**. This allows us to define the steady state force exerted by each population of motor

$$\tilde{F}^{\pm}(\tilde{v}) := \int_{-\infty}^{\infty} k^{\pm} x \tilde{m}(x; \tilde{v})\, dx, \tag{5}$$

where we are parameterizing this force as a function of the steady state cargo velocity $\tilde{v}$ which appears in (2.1).

We now need an equation governing the cargo velocity, which is determined by the forces exerted on the cargo

$$\mathcal{M}\dot{v} + \gamma v = \sqrt{2\gamma k_B T}\xi(t) + \text{forces exerted by motors}. \tag{6}$$

In (2.1), $\mathcal{M}$ is the mass of the cargo, γ is the drag coefficient of the cargo and $\xi(t)$ is the Wiener process due to thermal fluctuations (diffusion) of the cargo. The magnitude of these fluctuations is determined by the fluctuation-dissipation theorem [5].

2.2. Force Exerted By motors

A perhaps natural choice for the force terms in (2.1) could be taken to be the steady-state force, $\tilde{F}^{\pm}(v)$, found in (2.1), however there is a problem with this choice. Although v is changing instantaneously, the position of the cargo is not. The forces exerted by the motors are due to stretching of the linker, and therefore cannot change instantaneously as the velocity changes. Thus, parameterizing the force with time-varying velocity would not produce the physical behavior we desire. For this reason, we turn to a simpler model to understand what to use for the force terms in (2.1) that accounts for this issue.

In [2], the authors make the observation that including cargo noise produces this same difficulty: motors should not react instantaneously to velocity and classical models produce results inconsistent with experimental observations if this is the case. To overcome this issue, the authors hypothesize that the motors respond to a time-windowed-average force, suggesting some "memory" property of the motors. Here, we directly compute a physiological, mechanistic delay stemming from the stepping of the motor, instead of a phenomenological "memory".

2.2.1. Ornstein-Uhlenbeck motivation

To understand motor response to fluctuations in the cargo velocity, we now examine the behavior of a *single motor* on a *single run*: after binding and before unbinding. Let $x_1(t)$ be the random process describing the distance stretched the single motor is from its unstretched position and $p_1(x,t)$ be the probability density of this random variable. The behavior follows almost identically with the mean-field model (1.1), but now binding and unbinding can be neglected due to the analysis only being of a single run.

Thus, since this corresponds to a single run of a motor, the only remaining dynamics are the motor stepping (still at its force dependent velocity w) and diffusion (the magnitude of which is lumped into a parameter D). The resulting process is an Ornstein-Uhlenbeck process [5], which can be described by the Langevin equation

$$\dot{x}_1 = [w(x_1) - v(t)] + \sqrt{2D}\,\xi(t),$$

or the corresponding Fokker-Planck equation

$$\frac{\partial p_1}{\partial t} = -\frac{\partial}{\partial x}\left\{[w(x) - v(t)]p_1\right\} + D\frac{\partial^2 p_1}{\partial x^2}.$$

To quantify the motors ability to respond to instantaneous fluctuations in the cargo velocity, we consider the mean value of this single motor, single run process, denoted μ_1,

$$\mu_1 := \langle x_1(t) \rangle.$$

From the Fokker-Planck equation, we find the relationship describing the temporal evolution of the mean of this process to be (assuming w is a linear function)

$$\dot{\mu}_1 = w(\mu_1) - v(t). \tag{7}$$

For details of the calculation, see **Appendix A**.

However, again recalling the assumption of a Hookean force (that is, force $\sim kx_1$), the average force exerted by a single motor under evolving under this process with density $p(x_1, t)$ is then

$$F_{OU} = k \int_{-\infty}^{\infty} x_1 p(x_1, t) \, \mathrm{d}x_1 = k\mu_1. \tag{8}$$

In other words, *for a single motor, on a single run*, the force exerted can be parameterized by the mean distance stretched of the motor μ, where μ "tracks" the velocity through (2.2.1), which specifically specifies that the magnitude of the delay is determined by the motor velocity. This stems from the fact that changes in force are only due to changes in position, not velocity. This resolves the aforementioned issue about the force changing instantaneously. Now, the force tracks, with some delay as determined by (2.2.1), the velocity and evolves continuously.

2.2.2. Force Evolution Approximation

The previous calculation showed that while still attached, the force generated by individual motors (2.2.1) track instantaneous fluctuations in cargo velocity with a delay related to their processivity, described by (2.2.1). In other other words, the force generation for a population of motors could be collapsed down a single parameter μ_1. We now make the major approximation of the paper that even with binding and unbinding, the force generated by each population of motors can be collapsed to a single parameter μ (for each population) with a similarly structured delay. This leads us to the set of equations

$$\mathcal{M}\dot{v} + \gamma v = \hat{F}(\mu) + \sqrt{2\gamma k_B T}\xi(t), \qquad \dot{\mu} = w(\mu) - v. \tag{9}$$

Thus, the cargo velocity v evolves with the forces exerted on it, but the force exerted by the motors is not directly prescribed by the current v but rather some parameter μ which tracks v with a delay. We can regard μ as a "characteristic distance". That is, the force exerted by each population of motors is entirely parameterized by some dynamic variable μ, determined by $\hat{F}(\mu)$. This could be thought of as effectively the force exerted by a population of motors with mean position μ, staying in the spirit of the mean-field model. It is important to note that (2.2.2) is written for a single μ, meaning a single motor population to demonstrate the structure but we later incorporate a μ_1, μ_2, one for each population. We have also not yet specified the choice of $\hat{F}$ but rather are illustrating the structure of the dynamics.

Although the motivation for (2.2.2) was in the motor-attached scenario, the particular choice of $\hat{F}_j(\mu)$ (for $j = 1, 2$, corresponding to each population) must not neglect unbinding and binding of the motors incorporated in the mean-field model. Thus, we take the force exerted by the motors to be the steady state force generated, described by (2.1) such that

$$\hat{F}_j(\mu_j) = \tilde{F}_j(-a_j\mu_j + b_j). \tag{10}$$

We justify this by observing that $\tilde{F}$ was computed for motors equilibrated for a particular constant $\tilde{v}$, which we can think of this as when $\dot{\mu} = 0$ (that is, the mean position of the population is not changing), and therefore

$$\dot{\mu} = 0 = -a\mu + b - \tilde{v} \implies \tilde{v} = -a\mu + b,$$

meaning we associate $-a_j\mu_j + b_j$ with $\tilde{v}$ to obtain (2.2.2). This particular choice of the force structure allows for the complexity of the mean-field model, including all binding and unbinding to be embedded into the $\tilde{F}(\mu)$ terms. However, the dynamics of the reduced "characteristic position" model are easier to study due to being an ordinary differential equation rather than a partial differential equation.

To evaluate the validity of this approximation, we performed numerical simulations of the full mean-field model (1.1),(1.1) and the reduced model (2.2.2). For simplicity, we simulated only a single motor population (+ direction) and no thermal noise. The approximation fundamentally is one of how motors (and the force generated by them) respond temporally, so a numerical experiment was performed by applying instantaneous external forces to both the mean field model of motors and the reduced model, both of which have cargo dynamics determined by (2.1). Both models are started at the completely unloaded state and run to equilibrium. Once at equilibrium, a -5 pN force (and later +5 pN) external force is applied to the cargo for 5 ms and then removed. The mean-field PDE was simulated using a Lax-Wendroff scheme and the remaining ODEs used a Runge-Kutta 4(5) scheme. The dynamics of the force generated by the motor population and the resulting cargo velocity are tracked and shown in **Figure 2**.

From **Figure 2** we are able to make a number of observations about the validity of the "characteristic position" approximation. For one, the equilibria of the full model and reduced are the same, which is intuitive, given that the reduced model is built from the equilibrium of the full model, as described in (2.2.2). From this, we can conclude that there is agreement on long time scales. As the external force changes instantaneously, both models behave (quantitatively and qualitatively) similarly regardless of the directionality of the force, and therefore, also suggests agreement on short time scales. Other external inputs (e.g. sinusoid) were also investigated, but yielded similar results. Thus, we have collapsed the force generated by the PDE mean-field description of motors (1.1, 1.1) into an ODE (2.2.2) in a "characteristic position" variable and the approximation appears to be valid.

2.3. Full Model

The parameter regime we are considering deals with cargo with negligible mass, thus suggesting we are in a viscous or near-viscous regime. Exploiting this fact, we can perform an adiabatic (quasi-steady state) reduction on (2.2.2) to eliminate v. For details of this calculation,
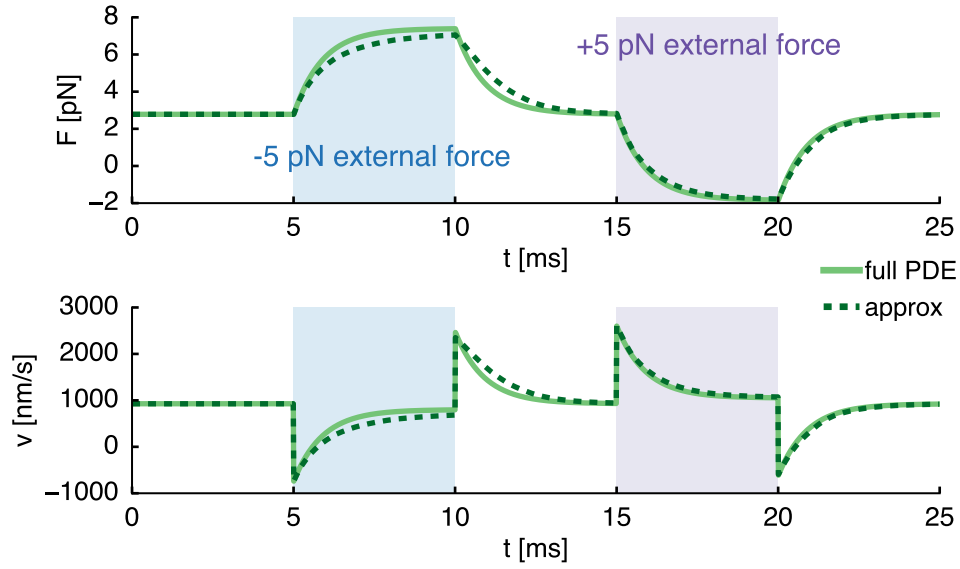
Figure 2: A numerical comparison of the forces and cargo velocity generated by the full mean field motor model (1.1, 1.1) with the "characteristic position" approximation described by (2.2.2) for one motor population and no thermal noise. In both models, the evolution of the cargo velocity is described by (2.1). External forces are applied to the cargo and removed to illustrate the ability of the reduced model to respond to temporal changes in force.

see **Supplementary Section S3**. The result of performing this reduction is

$$\dot{\mu} = w(\mu) - \frac{\hat{F}(\mu)}{\gamma} + \sqrt{\frac{2k_B T}{\gamma}} \xi(t),$$

or equivalently, in Fokker-Planck form

$$\frac{\partial p}{\partial t} = -\frac{\partial}{\partial \mu} \left\{ w(\mu) - \frac{1}{\gamma} \hat{F}(\mu) \right\} + \frac{k_B T}{\gamma} \frac{\partial^2 p}{\partial \mu^2}.$$

One important note from the calculation detailed in **Supplementary Section S3** is that although v is eliminated from the system, v relaxes quickly to a Gaussian centered around

$$\hat{v} \sim \hat{F}(\mu)/\gamma, \tag{11}$$

thus the value of μ directly determines the (mean) velocity of the cargo at any time.

Combining all of the previous observations, we now propose the full model. In the derivation of (**??**), only one motor population was considered, but in bidirectional transport, there are two populations evolving separately, resulting in two equations with identical structure but

different parameters. From this, we get the full model

$$\dot{\mu}_1 = -a_1\mu_1 + b_1 - \frac{1}{\gamma}\{F_1(\mu_1) + F_2(\mu_2)\} + \sqrt{\frac{2k_BT}{\gamma}}\xi(t),$$

$$\dot{\mu}_2 = -a_2\mu_2 + b_2 - \frac{1}{\gamma}\{F_1(\mu_1) + F_2(\mu_2)\} + \sqrt{\frac{2k_BT}{\gamma}}\xi(t).$$

(12)

Note that we have switched the two populations to labels $j = 1, 2$ instead of $+/-$ for notational convenience. We have also used the functional form of the motor force velocity curve $w(x) = -ax + b$ and that the net force exerted by the motors is simply the sum of the force exerted by each population.

F_{stall} [pN]	v_0 [nm·s^{-1}]	k_{off} [s^{-1}]	$|F_d|$ [pN]	k_{on} [s^{-1}]	M	k [pN·nm^{-1}]	γ [pN·s·nm^{-1}]
5	1000	1	1	5	10	0.4	0.001

Table 1: "Typical" motor values used for both populations of motors in the symmetric case of the mean field model. Values used are within reported ranges of kinesin and dynein.

To emphasize the ability of this model to produce bidirectional motion without asymmetry between the motor populations, we take the parameters describing each of the populations to be the same (unless noted otherwise), described in **Table 1**. These parameters are chosen as physiologically reasonable parameters in the range of reported values of both kinesin and dynein, taken from [15, 16, 27]. The viscosity of cytoplasm is reported to be higher than water [21, 23]. Although a potentially large viscosity is used in this work, any smaller would only make the magnitude of the fluctuations larger, further magnifying the importance of cargo diffusion.

2.4. Dimensional Reduction

An important observation must be made about the noise structure of (2.3): the white noise term in each equation is exactly the same (fully correlated). From a biophysical perspective, this is because the two motors feel the same fluctuations from the cargo diffusion. Hence, this is truly a one dimensional diffusion rather than two dimensional as it currently appears. The Fokker-Planck equation corresponding to the system (2.3) has a non-invertible diffusion tensor, which further illustrates this point. To make the one dimensional structure more apparent, we perform a change of variables, taking

$$\zeta := \mu_1 + \mu_2, \qquad \eta := \mu_1 - \mu_2 \qquad \Longrightarrow \qquad \mu_1 = \frac{1}{2}(\eta + \zeta), \qquad \mu_2 = \frac{1}{2}(\eta - \zeta).$$

Under this coordinate change, the system (2.3) becomes, abbreviating $D := k_BT/\gamma$

$$\dot{\zeta} = -\frac{a_1}{2}(\zeta + \eta) + b_1 - \frac{a_2}{2}(\zeta - \eta) + b_2 - \frac{2}{\gamma}\sum F + 2\sqrt{2D}\xi(t)$$

$$\dot{\eta} = -\frac{a_1}{2}(\zeta + \eta) + b_1 + \frac{a_2}{2}(\zeta - \eta) - b_2.$$

By taking the two populations to be symmetric, which corresponds to $a_1 = a_2 = a$ and $b_1 = -b_2 = b$, the η equation becomes

$$\dot{\eta} = -a\eta + 2b,$$

which has an invariant manifold described by $\tilde{\eta} = 2b/a$. Since the equilibria of the system must lie on this invariant manifold, all dynamics of interest evolve on the manifold and consequently reduces the problem to the one dimensional evolution

$$\dot{\zeta} = -a\zeta - \frac{2}{\gamma}\left[F_1\left(\frac{\zeta + \tilde{\eta}}{2}\right) + F_2\left(\frac{\zeta - \tilde{\eta}}{2}\right)\right] + 2\sqrt{2D}\xi(t), \tag{13}$$

where again, $\tilde{\eta}$ is the manifold described by $\tilde{\eta} = 2b/a$.

Thus, we have fully reduced the dynamics of the system to a single time-varying quantity ζ, which we again can be thought of as the *characteristic position* of the system. Although a considerable number of reductions have been made, the physical behavior of the system is still recoverable by recalling that the instantaneous mean cargo velocity of the system can be recovered from (2.3). In other words, $\zeta(t)$ is a proxy for $\hat{v}$, which is the biophysical quantity of interest.

3.   RESULTS AND DISCUSSION

3.1.   Metastable Behavior

We perform simulations of (2.4) with the parameters specified in **Table 1** with the Euler-Maruyama scheme [14]. The results of a typical simulation can be seen in **Figure 3**. From this simulation, we see a curious behavior: the characteristic position ζ switches between two configurations, or is said to be *metastable*. Elaborating on this, ζ takes on values near some particular point and then, due to the noise of the system, randomly switches to values centered around another point. The histogram of ζ values during the simulation, which can also be seen in **Figure 3** is clearly bimodal, which is a characteristic sign of metastability. Although the two peaks in the figure appear different, this is just a consequence of the short time for which the simulation was performed. If more switches were recorded, the two peaks of the histogram would be identical due to the symmetric population assumption.

The previous section illustrated the metastable behavior of the system, which we investigate further. To do so, consider the corresponding Fokker-Planck equation to (2.4), which describes the probability density $p(\zeta, t \,|\, \zeta_0, 0)$. That is, the probability density of (2.4) given that it started at ζ_0, which is described by

$$\partial_t p = -\partial_\zeta \left\{A(\zeta)p\right\} + 4D\partial_{\zeta\zeta}p, \tag{14}$$

where we are abbreviating

$$A(\zeta) := -a\zeta - \frac{2}{\gamma}\left[F_1\left(\frac{\zeta + \tilde{\eta}}{2}\right) + F_2\left(\frac{\zeta - \tilde{\eta}}{2}\right)\right], \qquad D := \frac{k_B T}{\gamma}. \tag{15}$$

Then, the potential can be defined by
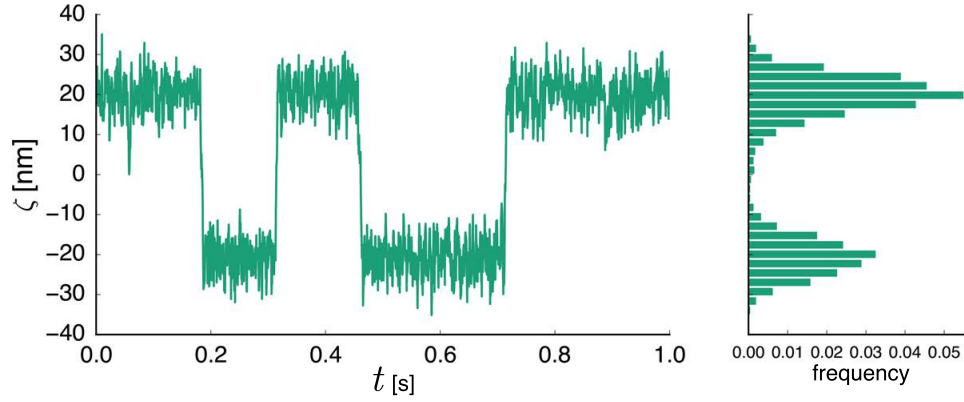
$$U(\zeta) := -\int A(\chi)\,\mathrm{d}\chi. \tag{16}$$

Figure 3: Left: A typical simulation of (2.4) performed with the Euler-Maruyama scheme. The system notably switches between two configurations. **Right:** A histogram of the values of the simulation, which demonstrates bimodality.

This potential $U(\zeta)$ is be plotted as a function of γ, the drag coefficient of the cargo and the result is can be seen in **Figure 4**. From the figure, we see that for a large range of γ values, the potential that ζ evolves in is a double-well potential. That is, there are two distinct well locations and a peak in the center, all three of which are roots of $A(\zeta)$. Denote the two well locations (stable fixed points of $A(\zeta)$) as ζ_{S1} and ζ_{S2}, where $\zeta_{S1} < \zeta_{S2}$ and the middle peak of the well (a hyperbolic fixed point of $A(\zeta)$) as ζ_H.

The effect of γ on the potential is non-trivial. Particularly, as γ decreases the wells deepen and also cause the wells to split farther apart, which alone, would suggest an increase in time to switch. However, we later see that there is a counteracting effect in the strength of diffusion.
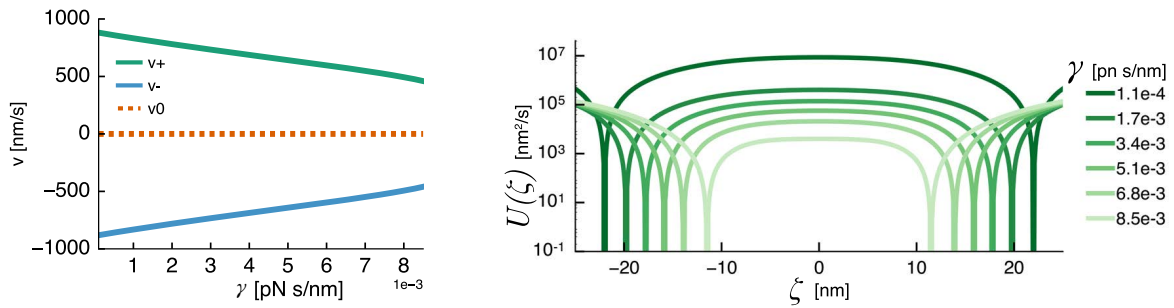

Figure 4: Left: The mean cargo velocities associated with the three equilibria of the system, determined by (2.3). The two metastable states correspond to positive and negative velocities, from which, bidirectionality of the system can be concluded. **Right:** the double-well potential structure (3.1) as a function of the drag coefficient γ. As γ decreases, the wells get steeper and farther apart.

The question remains: what, biophysically, do these two configurations represent? As mentioned in the previous section, ζ is a proxy for the mean cargo velocity at any given time. Thus, denote v_+, v_0, v_- to be the velocities associated with $\zeta_{S1}, \zeta_H, \zeta_{S2}$ respectively. The values of these velocities can be seen in **Figure 4** as a function of the drag, γ. In the figure, we see that the two metastable states correspond to a net positive or negative cargo velocity. Thus, the system

is bidirectional. It is also worth noting that the values of velocity produced are fairly robust to changes in γ and are also in a physiologically reasonable range [17].

3.2. Mean First Passage Time Analysis

One natural quantity to study in bidirectional systems is the time to switch directions, or the reversal time. By the double-potential well structure, this can be thought of as the mean time from one of the metastable points to the hyperbolic point, from which the system relaxes quickly to the other metastable point. Due to the symmetric motor population assumption, the time to switch states is independent of state. Thus, without loss of generality, we compute the mean first passage time from $\zeta_{S1} \to \zeta_{S2}$ where, again, $\zeta_{S1} < \zeta_H < \zeta_{S2}$.

The analysis of a mean first passage time in a one dimensional potential is classical [3, 5] and is be briefly summarized here. Define $G(z, t)$ to be the probability that the system described by (3.1) is in the leftmost potential well at time t given $p(\zeta, 0) = z$. That is, the survival probability density is described by

$$G(z, t) := \int_{\zeta_{S1}}^{\zeta_H} p(\zeta, t \mid z, 0) \, d\zeta.$$

Then, let $T(z)$ define the random variable describing the exit time from this potential well.

$$\mathbb{P}\left[T(z) < t\right] 1 - G(z, t). \tag{17}$$

Taking a derivative of (3.2) yields the density for exit time $f(z, t)$

$$f(z, t) = -\partial_t G(z, t) = -\int_{\zeta_{S1}}^{\zeta_H} \partial_t p(\zeta, t \mid z, 0) \, d\zeta.$$

From this, we can define the mean first exit time from the potential well, starting at the point z by

$$\tau(z) := \langle T(z) \rangle = \int_0^\infty t f(z, t) \, dt = \int_0^\infty (z, t) \, dt. \tag{18}$$

The survival probability $G(z, t)$ satisfies the backward Fokker-Planck equation [5], which we can integrate and use (3.2) to yield the governing equation for the mean exit time density of the system starting at $\zeta_0 = z$, which is

$$A(z)\tau' + 4D\tau'' = -1, \qquad \tau(\zeta_H) = 0, \qquad \tau'(\zeta_{S1}) = 0. \tag{19}$$

The reflecting boundary at ζ_{S1} is a consequence of starting starting the system in the well corresponding to this point, as any excursions to the left will quickly relax back to the bottom of the well. The exit location, the hyperbolic point ζ_H, is an absorbing state due to the fast relaxation to the other potential well once the system transverses the peak between them.

The boundary value problem (3.2) does not appear to be solvable analytically due to the complexity of the force curves. However, $\tau(z)$ can be computed numerically in a straightforward manner (in a single integration) by exploiting the linearity of the system. Alternatively, a deep-well approximation can be made for the potential and the classical *Arrhenius formula* can be

used to approximate the mean first passage time. For details on both of these methods, see **Appendix: 5.2**.

The two aforementioned techniques of evaluating $\tau(\zeta_{S1})$ are computed and compared against Monte Carlo simulations of (2.4), again using the Euler-Maruyama scheme, where switching is considered passing the hyperbolic point. The result of these techniques can be seen in **5**. From this, we see that the shooting technique agrees with Monte Carlo simulations and the deep-well approximation is, although qualitatively similar, an overestimate of the switching time. This result is intuitive, as in reality, the wells may not be sufficiently deep for the approximation to work well and therefore allow escape much faster.
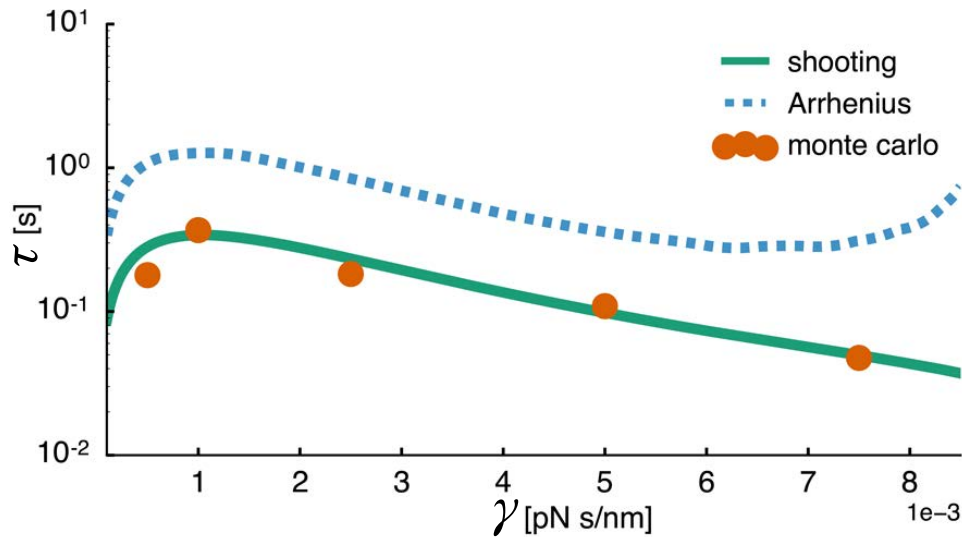

Figure 5: Mean first passage times corresponding to the cargo switching directions. Two approaches to solving (3.2) are illustrated: a shooting technique, and the deep-well Arrhenius approximation. The results of an Euler-Maruyama simulation of (2.4) are also shown, where switching is considered passing through the hyperbolic point.

The behavior of the mean first passage times as a function of the drag, γ is quite interestingly, non-monotonic. That is, as the drag coefficient increases (which can be thought of as the cargo increasing in size), the time to switch initially goes up, but then ultimately goes back down. Mathematically, this complexity stems from γ scaling both the potential and the diffusion strength, as in (3.1). As γ decreases, the potential wells deepen and spread apart, but the strength of diffusion simultaneously goes up, which are competing effects for the switching time. The resulting behavior, or which "wins" is therefore complex and produces this non-monotonicity.

From a biophyiscal perspective, it should be noted that the predicted mean first passage times are on the order of ~ 0.5[s], which agrees with experimentally observed values [17], which supports the hypothesis that cargo diffusion is the noise source for bidirectionality. The non-monotonicity of the curve also provides a verifiable, experimental prediction. That is, bidirectional motion via molecular motors could be observed for different cargo drag values (which, could be obtained by varying bead size). If the resulting mean time to switch directions is found to be non-monotonic, this would support our claim that cargo diffusion, not motor binding dy-

namics are indeed the noise source of bidirectionality.

4. CONCLUSION & DISCUSSION

In this work, we have proposed a mean-field, unequally distributed load description of motor-mediated transport. To understand the behavior of this complex model, we perform a series of reductions. The first, inspired by a simple Ornstein-Uhlenbeck process, quantifies the delay in which motors are able to respond to instantaneous changes in the cargo velocity. Secondly, we use the small mass of the cargo to perform an adiabatic (quasi-steady state) reduction of the system. Due to the correlated noise structure, the final system describes the dynamics of a single "characteristic position" which is a proxy for the instantaneous cargo velocity. This resulting stochastic dynamics are observed to be "metastable", switching between two distinct states exclusively due of cargo diffusion. These states are associated with positive and negative cargo velocities, meaning the system is bidirectional. To quantify the reversal time of the system, a mean-first passage time analysis is performed and the results are explored as a function of the cargo drag, an experimentally tunable quantity. Ultimately, we find that the predicted switching time agrees with experimental values and also has an interesting non-monotonic shape, a claim that can be experimentally verified.

The Ornstein-Uhlenbeck analysis for quantifying the ability of a motor to react to instantaneous changes in cargo velocity is of interest in other recent works [2]. In this paper, the authors hypothesize a "motor memory" and conclude that models only agree with experimental values appropriately if the motors react to a windowed-time-average velocity. In our work, we have quantified this "memory" directly from the physiology of the motor. However, our analysis was only performed for a single motor and was assumed to hold for a population. Thus, quantifying this reaction for a whole population is still desirable.

In [2], the authors also cite the importance of cargo diffusion in models producing results that match experimental values. In our work, we have further illustrated the importance of cargo diffusion by illustrating its ability to produce qualitative changes in motor-mediated transport. Specifically, the fundamental noise driving switching in our model is cargo diffusion, unlike previous unequally distributed load models which depended on a discrete motor description. This raises the possibility of the importance of diffusion in other aspects of motor-mediated transport.

Thus, we have illustrated that common features of previous work: discreteness of the motors, asymmetry of motor populations, equally distributed loads are *not* necessary to produce a physiologically reasonable model of bidirectional motor transport. This raises uncertainty of which key ingredients may be essential for tug-of-war, making it even more difficult to compare to the alternative regulatory hypothesis of bidirectionality. However, in our work, we have provided an experimental prediction of the reversal time as a function of the drag coefficient, which can be tuned by the bead size in experimental setups. If indeed thermal noise is the driver of this switching, then agreement with this experiment would support this claim.

5. APPENDIX

5.1. Ornstein-Uhlenbeck Mean Evolution

In this section, we show that if the advection term of an Ornstein-Uhlenbeck has a time dependence, a differential equation can be obtained for the mean of the process, demonstrating an effective delay.

Consider a Fokker-Planck equation of the form

$$\partial_t p = -\partial_x \left[\{w(x) - v(t)\} \, p \right] + D\partial_{xx}p. \tag{20}$$

Denote $\mu(t)$ to be the mean of the process, that is $\mu = \langle p \rangle$. Then, we have:

$$\dot{\mu} = \frac{\mathrm{d}}{\mathrm{d}t} \int_{-\infty}^{\infty} x \, p(x,t) \, \mathrm{d}x = \int_{-\infty}^{\infty} x\partial_t p \, \mathrm{d}x.$$

However, we can use (5.1) to find that

$$\dot{\mu} = - \int_{-\infty}^{\infty} x\partial_x \left[\{w(x) - v(t)\} \, p \right] \, \mathrm{d}x + \int_{-\infty}^{\infty} xD\partial_{xx}p \, \mathrm{d}x,$$

which, after integration by parts, yields

$$\dot{\mu} = \langle w(x) \rangle - v.$$

Jensen's inequality states that for a convex w

$$\langle w(x) \rangle \geq w(\langle x \rangle),$$

however, if we assume $w(x)$ is *linear* (as we have done in the model), then Jensen's inequality attains equality and the result is

$$\dot{\mu} = w(\mu) - v(t).$$

5.2. Methods for 1D MFPT Problems

For the sake of generality, consider the 1D SDE

$$\mathrm{d}x = A(x)\mathrm{d}t + \sqrt{2B(x)} \, \mathrm{d}W,$$

which has a corresponding Fokker-Planck equation

$$\partial_t p = -\partial_x \{A(x)\} + B(x)\partial_{xx}p.$$

We are assuming that $A(x)$ has three fixed points, two stable and one hyperbolic, which we'll denote x_S and x_H.

We are then interested in the mean first passage time starting from a point y, which we'll denote $\tau(y)$, which satisfies

$$A(y)\tau' + B(y)\tau'' = -1, \qquad \tau'(x_S) = 0, \qquad \tau(x_H) = 0. \tag{21}$$

5.2.1. Shooting Method

In this section, we exploit the lineariy of (5.2) to construct a numerical shooting method for constructing a solution. First, we write the system as a first order system, by taking $\sigma = \tau'$, meaning we have

$$\begin{bmatrix} \tau' \\ \sigma' \end{bmatrix} + \begin{bmatrix} 0 & 1 \\ 0 & \frac{A(x)}{B(x)} \end{bmatrix} \begin{bmatrix} \tau \\ \sigma \end{bmatrix} = \begin{bmatrix} 0 \\ -\frac{1}{B(x)} \end{bmatrix}, \qquad \begin{bmatrix} \tau(x_H) \\ \sigma(x_S) \end{bmatrix} = \begin{bmatrix} 0 \\ 0 \end{bmatrix}. \tag{22}$$

To construct a solution to (5.2.1), we obtain two solutions of initial value problems of the same form and utilize the linearity of the equation to solve the boundary value problem via superposition. Thus, consider the following two systems:

$$\begin{bmatrix} p_1' \\ p_2' \end{bmatrix} + \begin{bmatrix} 0 & 1 \\ 0 & \frac{A(x)}{B(x)} \end{bmatrix} \begin{bmatrix} p_1 \\ p_2 \end{bmatrix} = \begin{bmatrix} 0 \\ -\frac{1}{B(x)} \end{bmatrix}, \qquad \begin{bmatrix} p_1(x_S) \\ p_2(x_S) \end{bmatrix} = \begin{bmatrix} 0 \\ 0 \end{bmatrix}$$

$$\begin{bmatrix} q_1' \\ q_2' \end{bmatrix} + \begin{bmatrix} 0 & 1 \\ 0 & \frac{A(x)}{B(x)} \end{bmatrix} \begin{bmatrix} q_1 \\ q_2 \end{bmatrix} = \begin{bmatrix} 0 \\ 0 \end{bmatrix}, \qquad \begin{bmatrix} q_1(x_S) \\ q_2(x_S) \end{bmatrix} = \begin{bmatrix} 1 \\ 0 \end{bmatrix}$$

We now claim $\Upsilon = \begin{bmatrix} \tau & \sigma \end{bmatrix}^T$ is a linear combination of $P = \begin{bmatrix} p_1 & p_2 \end{bmatrix}^T$ and $Q = \begin{bmatrix} q_1 & q_2 \end{bmatrix}^T$. In other words, there exists some γ such that $\Upsilon = P + \gamma Q$. The value of γ is to be determined by making sure the right boundary condition is satisfied

$$\tau(x_H) = p_1(x_H) + \gamma q_1(x_H) = 0 \implies \gamma = -\frac{p_1(x_H)}{q_1(x_H)}.$$

Thus, our mean first passage time from $x_S \to x_H$ is then

$$\tau(x_S) = p_1(x_S) + \gamma q_1(x_S) = \gamma.$$

It is worth noting that this actually only requires a *single* ODE integration, as Q is identically constant by construction with $q_1 \equiv 1$ and $q_2 \equiv 0$, and consequently

$$\gamma = -p_1(x_H).$$

5.2.2. Arrhenius (Deep Well) Approximation

The deep-well approximation is a classical technique used to approximate the solution to a mean-first passage time boundary value problem for a double-well potential. Here, we briefly summarize the result but additional details can be found in [3, 5]. Define the potential function $U'(y) := A(y)$, so $U = \int A(y)\,\mathrm{d}y$, then, after using an integrating factor and assuming B is constant for simplicity, we have

$$\tau = \frac{1}{B} \int_{x_S}^{x} e^{U(x')/B}\,\mathrm{d}x' \int_{0}^{x'} e^{-U''(x'')/B}\,\mathrm{d}x''.$$

Assuming the potential is deep-welled, the first integral is dominated around the region $x'' = x_S$ and the second dominated by $x' = x_0$, which allows the limits to be changed with small error and therefore can be approximated by

$$\tau = \frac{1}{B} \left[\int_{-\infty}^{\infty} e^{-U(x'')/B} \, \mathrm{d}x'' \right] \left[e^{U(x')/B} \, \mathrm{d}x' \right].$$

Using the method of steepest descent (or simply, Taylor expansion), we finally have the classical *Arrhenius formula*

$$\tau \sim \frac{2\pi}{\sqrt{|U''(x_H)|U''(x_S)}} e^{(\Delta U)/B}, \qquad \Delta U := U(x_H) - U(x_S).$$

References

[1] M Badoual, F. Julicher, and J Prost. "Bidirectional cooperative motion of molecular motors." *Proc. Natl. Acad. Sci.* 99.10 (2002) (cit. on p. 1).

[2] S. Bouzat. "Models for microtubule cargo transport coupling the Langevin equation to stochastic stepping motor dynamics: Caring about fluctuations." *Phys. Rev. E* 93.1 (2016) (cit. on pp. 2, 4, 6, 15).

[3] P. C. Bressloff. "Stochastic Processes in Cell Biology." Vol. 41. Interdisciplinary Applied Mathematics. Springer International Publishing, 2014 (cit. on pp. 13, 17).

[4] M.-M. Fu, and E. L. F. Holzbaur. "Integrated regulation of motor-driven organelle transport by scaffolding proteins." *Trends Cell Biol.* 24.10 (2014) (cit. on p. 1).

[5] C. Gardiner. "Stochastic Methods: A Handbook for the Natural and Social Sciences." 4th. Vol. 13. Springer Series in Synergetics. Springer Berlin Heidelberg, 2009 (cit. on pp. 6, 13, 17).

[6] A. Gennerich, A. P. Carter, S. L. Reck-Peterson, and R. D. Vale. "Force-Induced Bidirectional Stepping of Cytoplasmic Dynein." *Cell* 131.5 (2007) (cit. on p. 4).

[7] T. Guérin, J. Prost, and J.-F. Joanny. "Bidirectional motion of motor assemblies and the weak-noise escape problem." *Phys. Rev. E* 84.4 (2011) (cit. on p. 2).

[8] W. O. Hancock. "Bidirectional cargo transport: moving beyond tug of war." *Nat. Rev. Mol. Cell Biol.* 15.9 (2014) (cit. on p. 1).

[9] A. G. Hendricks et al. "Motor Coordination via a Tug-of-War Mechanism Drives Bidirectional Vesicle Transport." *Curr. Biol.* 20.8 (2010) (cit. on p. 1).

[10] J. Howard. "Mechanics of Motor Proteins and the Cytoskeleton." Sinauer Associates, 2001 (cit. on p. 1).

[11] A. F. Huxley. "Muscle structure and theories of contraction." *Prog. Biophys. Biophys. Chem.* 7 (1957) (cit. on p. 4).

[12] K. Kawaguchi, S. Uemura, and S. Ishiwata. "Equilibrium and Transition between Single- and Double-Headed Binding of Kinesin as Revealed by Single-Molecule Mechanics." *Biophys. J.* 84.2 (2003) (cit. on pp. 4, 5).

[13] J. P. Keener and J. Sneyd. "Mathematical Physiology." Springer Science & Business Media, 2008 (cit. on p. 4).

[14] P. E. Kloeden and E. Platen. "Numerical Solution of Stochastic Differential Equations." Vol. 23. Stochastic Modelling and Applied Probability 1. Springer, 1992 (cit. on p. 11).

[15] S. Klumpp, F. Berger, and R. Lipowsky. "Molecular Motors: Cooperative Phenomena of Multiple MolecularMotors." *Multiscale Model. Biomech. Mechanobiol.* Ed. by S. De, W. Hwang, and E. Kuhl. Springer London, 2015. Chap. 3 (cit. on p. 10).

[16] A. Kunwar, M. Vershinin, J. Xu, and S. P. Gross. "Stepping, Strain Gating, and an Unexpected Force-Velocity Curve for Multiple-Motor-Based Transport." *Curr. Biol.* 18.16 (2008) (cit. on pp. 1, 4, 10).

[17] A. Kunwar et al. "Mechanical stochastic tug-of-war models cannot explain bidirectional lipid-droplet transport." *Proc. Natl. Acad. Sci.* 108.47 (2011) (cit. on pp. 2, 4, 5, 13, 14).

[18] C. B. Lindemann and A. J. Hunt. "Does axonemal dynein push, pull, or oscillate?" *Cell Motil. Cytoskeleton* 56.4 (2003) (cit. on p. 4).

[19] R. Lipowsky et al. "Molecular motor traffic: From biological nanomachines to macroscopic transport." *Phys. A Stat. Mech. its Appl.* 372.1 (2006) (cit. on p. 2).

[20] R. Lipowsky et al. "Cooperative behavior of molecular motors: Cargo transport and traffic phenomena." *Phys. E Low-dimensional Syst. Nanostructures* 42.3 (2010) (cit. on p. 2).

[21] K Luby-Phelps. "Cytoarchitecture and physical properties of cytoplasm: volume, viscosity, diffusion, intracellular surface area." *Int. Rev. Cytol.* 192 (2000) (cit. on p. 10).

[22] R. J. McKenney et al. "LIS1 and NudE Induce a Persistent Dynein Force-Producing State." *Cell* 141.2 (2010) (cit. on p. 2).

[23] C. S. Mitchell and R. H. Lee. "A quantitative examination of the role of cargo-exerted forces in axonal transport." *J. Theor. Biol.* 257.3 (2009) (cit. on p. 10).

[24] M. J. Müller, S. Klumpp, and R. Lipowsky. "Tug-of-war as a cooperative mechanism for bidirectional cargo transport by molecular motors." *Proc. Natl. Acad. Sci.* 105.12 (2008) (cit. on pp. 2, 4).

[25] B. Nadrowski, P. Martin, and F. Julicher. "Active hair-bundle motility harnesses noise to operate near an optimum of mechanosensitivity." *Proc. Natl. Acad. Sci.* 101.33 (2004) (cit. on p. 2).

[26] O. Osunbayo et al. "Cargo transport at microtubule crossings: Evidence for prolonged tug-of-war between kinesin motors." *Biophys. J.* 108.6 (2015) (cit. on p. 1).

[27] M. J. Schnitzer, K. Visscher, and S. M. Block. "Force production by single kinesin motors." *Nat. Cell Biol.* 2.10 (2000) (cit. on p. 10).

[28] M. Shojania Feizabadi et al. "Microtubule C-Terminal Tails Can Change Characteristics of Motor Force Production." *Traffic* 16.10 (2015) (cit. on p. 2).

[29] V. Soppina et al. "Tug-of-war between dissimilar teams of microtubule motors regulates transport and fission of endosomes." *Proc. Natl. Acad. Sci. U. S. A.* 106.46 (2009) (cit. on p. 2).

[30] M. Srinivasan and S. Walcott. "Binding site models of friction due to the formation and rupture of bonds: State-function formalism, force-velocity relations, response to slip velocity transients, and slip stability." *Phys. Rev. E - Stat. Nonlinear, Soft Matter Phys.* 80.4 (2009) (cit. on p. 4).

Supplemental Information

Bidirectionality From Cargo Thermal Fluctuations in Motor-Mediated Transport

C E. Miles, J P. Keener

S1. Steady-State Force Density

In this section, we construct an analytical solution to the steady-state mean field equation (2.1) with the particular choice of functional forms described in the chapter. Thus, we are looking at equations of the form

$$\partial_x \left\{ (w(x) - v)m \right\} + k_{\text{off}} e^{k|x|/F_D} m = \left\{ M - \int_{-\infty}^{\infty} m(x)\, \mathrm{d}x \right\} k_{\text{on}} \delta(x).$$

The first observation that can be made is: due to the linearity of this equation, we can reduce it to the study of the simpler equation

$$\partial_x \left\{ (w(x) - v)u \right\} + k_{\text{off}} e^{k|x|/F_D} u = k_{\text{on}} \delta(x), \tag{S1}$$

where $m(x)$, the original solution can be recovered via the relationship

$$m(x) = \frac{M}{1+U} u(x), \qquad U := \int_{-\infty}^{\infty} u(x)\, \mathrm{d}x.$$

We now divide everything through by k_{off} in (S1) and recall $w(x) = -ax + b$. Denote the rescaled variables $\cdot/k_{\text{off}}$ by $\tilde{\cdot}$ and also abbreviate $k/FD = \alpha$, yielding

$$\partial_x \left\{ (-\tilde{a}x + \tilde{b} - \tilde{v})u \right\} + \exp\{\alpha|x|\}u = \tilde{k}\delta(x). \tag{S2}$$

We can now split this into two scenarios: to the left of $x = 0$ and to the right:

$$\begin{cases} \partial_x \left\{ (-\tilde{a}x + \tilde{b} - \tilde{v})u_L \right\} + \exp\{-\alpha x\}u_L = 0 & \text{for } x < 0, \\ \partial_x \left\{ (-\tilde{a}x + \tilde{b} - \tilde{v})u_R \right\} + \exp\{\alpha x\}u_R = 0 & \text{for } x > 0. \end{cases} \tag{S3}$$

These two equations must satisfy a matching condition at $x = 0$, so consider integrating (S1) a tiny window around $x = 0$ from $-\varepsilon$ to ε, yielding

$$\int_{-\varepsilon}^{\varepsilon} \partial_x \left\{ (-\tilde{a}x + \tilde{b} - \tilde{v})u \right\} + \exp\{\alpha|x|\}u = (b - v)\left[u_R(0) - u_L(0)\right] \quad = \quad \int_{-\varepsilon}^{\varepsilon} \tilde{k}\delta(x)\, \mathrm{d}x = \tilde{k}.$$

In other words, we have the matching condition

$$(b - v)\left[u_R(0) - u_L(0)\right] = \tilde{k}.$$

Integrating (S1), we find

$$u_L(x) = \frac{\alpha_L}{\tilde{a}x - \tilde{b} + \tilde{v}} \exp\left\{ \frac{1}{\tilde{a}} \exp\left(\frac{(-\tilde{b} + \tilde{v})\alpha}{a} \right) \mathrm{Ei}\left(-\frac{(-\tilde{b} + \tilde{v} + \tilde{a}x)}{\tilde{a}} \right) \right\}$$

$$u_R(x) = \frac{\alpha_R}{\tilde{a}x - \tilde{b} + \tilde{v}} \exp\left\{ \frac{1}{\tilde{a}} \exp\left(\frac{(\tilde{b} - \tilde{v})\alpha}{a} \right) \mathrm{Ei}\left(\frac{(-\tilde{b} + \tilde{v} + \tilde{a}x)}{\tilde{a}} \right) \right\},$$

where α_R, α_L are unknown constants and Ei is the exponential integral. The matching of these two can be simplified by the realization: only one of u_L, u_R is non-zero.

That is, if $-\tilde{a}x + \tilde{b} - v > 0$, then the advection is rightward (only starting from $x = 0$) and therefore $u_L = 0$. Similarly, if the advection is leftward then $u_R = 0$ necessarily. It should also be noted that (S1) demonstrate the integrable singularity at $x^\star = \frac{-\tilde{v}+\tilde{b}}{\tilde{a}}$, beyond this point, the solution is also necessarily zero. Thus, the solution reduces to either the interval $[0, x^\star]$ or $[x^\star, 0]$ depending on the sign of $x^\star$, or really, if $b > v$.

Thus, if $b > v$, then $x^\star > 0$ and $u_L < 0$ and if $b < v$ then $x^\star < 0$ and $u_R = 0$. Thus, if $b > v$, then our matching condition provides us α_R:

$$\alpha_R = -\tilde{k} \exp\left\{ \frac{1}{\tilde{a}} \exp\left(\frac{(\tilde{b} - \tilde{v})\alpha}{\tilde{a}} \right) \text{Ei}\left(\frac{(-\tilde{b} + \tilde{v})\alpha}{\tilde{a}} \right) \right\}.$$

Similarly, in the case that $b < v$, we have

$$\alpha_L = \tilde{k} \exp\left\{ \frac{1}{\tilde{a}} \exp\left(\frac{(-\tilde{b} + \tilde{v})\alpha}{\tilde{a}} \right) \text{Ei}\left(\frac{(\tilde{b} - \tilde{v})\alpha}{\tilde{a}} \right) \right\}.$$

Thus, we have constructed all components of the analytical solution to the original steady state equation.

S2. Force-Velocity Curves

In this section, we plot the steady state force-velocity curves described by (1.1). In these plots, the parameter values are taken to be those described by **Table 1** except for one parameter (shown in the legend), which is adjusted over a range of values.
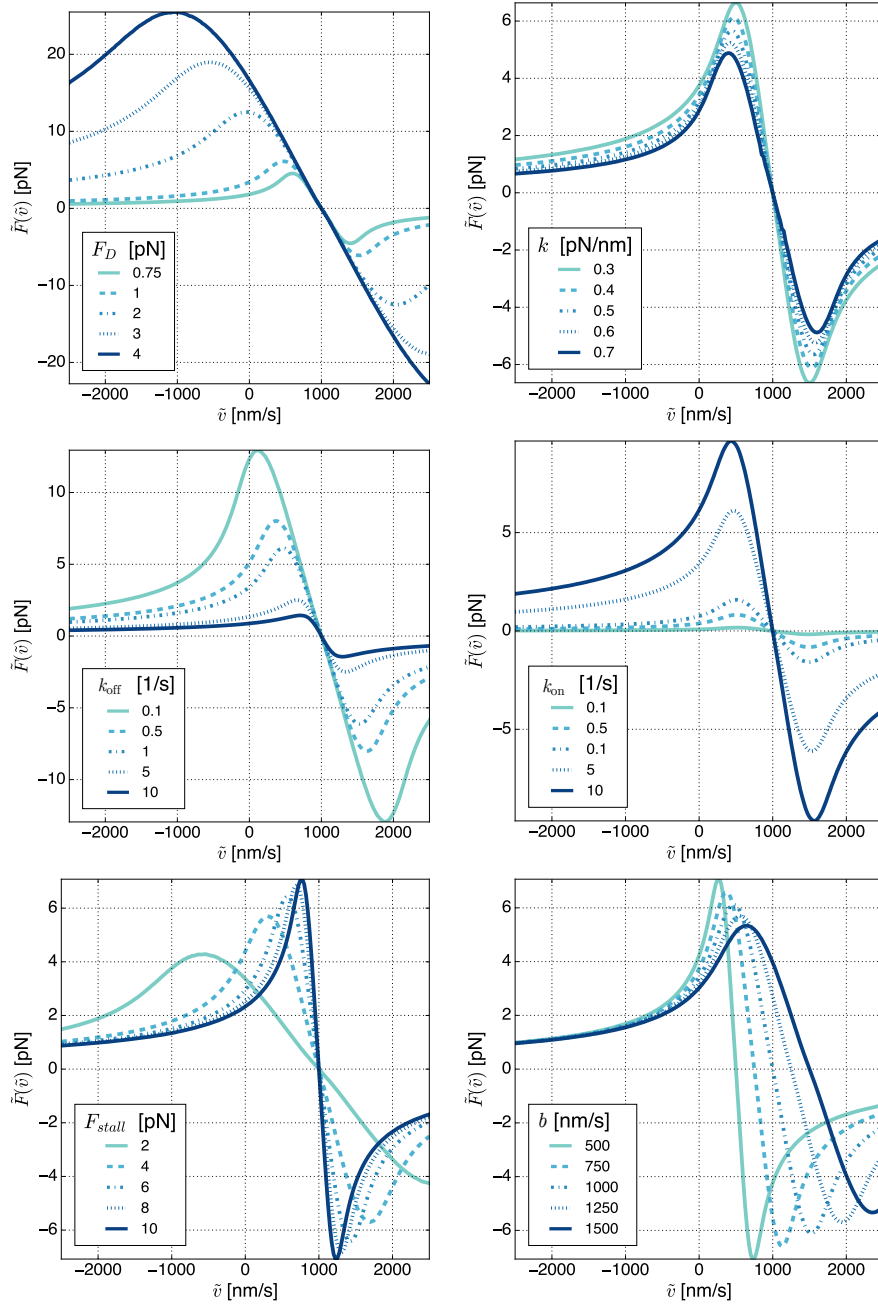

Figure S1: Plots of the steady state force distribution $\tilde{F}$ parameterized by the velocity of the cargo for different parameter values.

S3. Adiabatic Reduction Details

In this section, we perform an adiabatic reduction of (2.2.2), which, recalling the form of $w(x)$ and using $F(x) = kx$ for the sake of illustration, yields

$$\mathcal{M}\dot{v} + \gamma v = kx + \sqrt{2\gamma k_B T}\xi(t), \qquad \dot{x} = ax + b - v,$$

which is equivalent to the Fokker-Planck equation

$$\frac{\partial p}{\partial t} = -\frac{\partial}{\partial x}\left\{(ax + b - v)p\right\} - \frac{1}{\mathcal{M}}\frac{\partial}{\partial v}\left\{(kx - \gamma v)p\right\} + \frac{k_B T\gamma}{\mathcal{M}^2}\frac{\partial^2 p}{\partial v^2}. \tag{S5}$$

We first perform a non-dimensionalization. Let $y = x/x_0, \tau = t/t_0$, which provides a scaling on the velocity $u = vt_0/x_0$, all of which are dimensionless, where we particularly take $t_0 = \gamma/k$, and set $\gamma t_0/\mathcal{M} = 1/\varepsilon$, which gives us that $\gamma^2/k\mathcal{M} = 1/\varepsilon$. We can then also set the last term $\gamma k_B T t_0^2/\mathcal{M}^2 x_0^2 = 1/\varepsilon$, which gives us that $x_0 = \sqrt{k_B T\gamma^2/\mathcal{M}k^2}$. Then, (S3) becomes

$$\frac{\partial p}{\partial \tau} = -\frac{\partial}{\partial y}\left\{(\alpha y + \beta - u)\,p\right\} + \frac{1}{\varepsilon}\frac{\partial}{\partial u}\left\{(u - y)p + \frac{\partial p}{\partial u}\right\},$$

which we denote

$$\frac{\partial p}{\partial \tau} = \frac{1}{\varepsilon}\mathbb{L}_1 p + \mathbb{L}_2 p.$$

Note, the null-space of the fast operator, $\mathbb{L}_1$ is **not** the same as the classical Brownian due to a different choice of ε.

Now, if $\phi \in \mathrm{null}(\mathbb{L}_1)$, then it satisfies the following differential equation:

$$\frac{\partial \phi}{\partial u} + (u - y)\phi = 0,$$

which has a solution

$$\phi(u) = \frac{1}{\sqrt{2\pi}}\exp\{-(u - y)^2/2\}.$$

Define the projection operator $\mathbb{P}$ as

$$\mathbb{P}f := \phi(u, y)\int_{-\infty}^{\infty} f(u, y)\,\mathrm{d}u, \qquad \mathbb{Q} := 1 - \mathbb{P}.$$

We then split our solution p into the part in the null-space of the fast operator and otherwise. That is,

$$p = \mathbb{P}p + \mathbb{Q}p = v + w,$$

where we take v to be of the form $v = f(y, t)\phi(u, y)$, as it is in the null space of $\mathbb{L}_1$, and f is some unknown amplitude.

We first consider applying $\mathbb{L}_2$ to v for later calculations

$$\mathbb{L}_2 v = \mathbb{L}_2\mathbb{P}p = -\frac{\partial}{\partial y}\left\{(\alpha y + \beta - u)\,f(y)\phi(u, y)\right\}.$$

Now, applying $\mathbb{P}$ to this result yields

$$\mathbb{P}\mathbb{L}_2\mathbb{P}p = -\frac{\partial}{\partial y}\left\{(\alpha y + \beta - y)f\right\}\phi(u, y).$$

Next, we consider applying $\mathbb{P}$ and $\mathbb{Q}$ to the Fokker-Planck equation to yield the differential equation

$$\mathbb{P}\left(\frac{\partial p}{\partial \tau}\right) = \frac{\partial v}{\partial \tau} = \mathbb{P}\left(\frac{1}{\varepsilon}\mathbb{L}_1 + \mathbb{L}_2\right)(v + w) = \mathbb{P}\mathbb{L}_2 v + \mathbb{P}\mathbb{L}_2 w = -\frac{\partial}{\partial y}\left\{(\alpha y + \beta - y)f\right\}\phi + \mathbb{P}\mathbb{L}_2 w,$$

based on the first calculation and the fact that $\mathbb{P}\mathbb{L}_1 = 0$ by construction. Next, we have

$$\mathbb{Q}\left(\frac{\partial p}{\partial \tau}\right) = \frac{\partial w}{\partial \tau} = \mathbb{Q}\left(\frac{1}{\varepsilon}\mathbb{L}_1 + \mathbb{L}_2\right)(v + w)$$

$$= \frac{1}{\varepsilon}\mathbb{L}_1 w + \mathbb{Q}\mathbb{L}_2(v + w)$$

$$= \frac{1}{\varepsilon}\mathbb{L}_1 w + \mathbb{L}_2 v + \mathbb{L}_2 w - \mathbb{P}\mathbb{L}_2 v - \mathbb{P}\mathbb{L}_2 w.$$

Noting that, again $\mathbb{P}\mathbb{L}_1 = 0$ and $\mathbb{L}_1 v = 0$ by construction. We now take w to be in quasi-steady state, meaning it must satisfy

$$\frac{1}{\varepsilon}\mathbb{L}_1 w = -\mathbb{L}_2 v + \mathbb{P}\mathbb{L}_2 v,$$

which, when using the definitions of these operators yields

$$\frac{1}{\varepsilon}\frac{\partial}{\partial u}\left\{(u - y)w + \frac{\partial w}{\partial u}\right\} = \frac{\partial}{\partial y}\left\{(\alpha y + \beta - u)\,f(y)\phi(u, y)\right\} - \frac{\partial}{\partial y}\left\{(\alpha y + \beta - y)f\right\}\phi(u, y).$$

We integrate once with respect to u to get rid of a derivative on the left hand side, finding that

$$\frac{1}{\varepsilon}\left\{(u - y)w + \frac{\partial w}{\partial u}\right\} = \phi\left\{f(y)(u - \alpha y - \beta) + f'\right\}.$$

and therefore, using an integrating factor

$$w = \frac{\varepsilon}{2}\phi u\left\{f(y)(u - 2\alpha y - 2\beta) + 2f'(y)\right\}.$$

Now, using this form of w, we must compute $\mathbb{P}\mathbb{L}_2 w$, since that is the term in the $\partial v/\partial t$ equation. First, applying $\mathbb{L}_2$, by definition:

$$\mathbb{L}_2 w = -\frac{\partial}{\partial y}\left\{(\alpha y + \beta - u)\,w(u, y)\right\}.$$

and now projecting yields

$$\mathbb{P}\mathbb{L}_2 w = \varepsilon\left[f(y) + yf'(y) + f''(y)\right]\phi(u).$$

Thus, our differential equation for v is

$$\frac{\partial v}{\partial \tau} = -\varepsilon\frac{\partial}{\partial y}\left\{(\alpha y + \beta)f\right\} + \mathbb{P}\mathbb{L}_2 w = -\varepsilon\frac{\partial}{\partial y}\left\{(\alpha y + \beta)f\right\} + \varepsilon\left[f(y) + yf'(y) + f''(y)\right]\phi(u),$$

from which, we can conclude

$$\frac{\partial f}{\partial \tau} = -\varepsilon \frac{\partial}{\partial y}\left\{(\alpha y + \beta)f\right\} + \varepsilon \frac{\partial}{\partial y}\left\{yf(y)\right\} + \varepsilon \frac{\partial^2 f}{\partial y^2},$$

in the original variables,

$$\frac{\partial f}{\partial t} = -\frac{\partial}{\partial x}\left\{\left(ax + b - \frac{k}{\gamma}x\right)f(x)\right\} + \frac{k_B T}{\gamma}\frac{\partial^2 f}{\partial x^2}.$$